J Nanostruct 15(4): 1979-1993, Autumn 2025

RESEARCH PAPER

Investigation of Photocatalytic Activity of the Synthesized Nickel Oxide with Cobalt Oxide Nanocomposites via Removing of Malachite Green Dye from Aqueous Solution

Alaa Salman Hussein [1]*, *Abbas Jasim Atiyah* [2]

[1] College of Dentistry, University of Babylon, Iraq

[2] College of Sciences, University of Babylon, Iraq

ARTICLE INFO

Article History:
Received 07 May 2025
Accepted 21 September 2025
Published 01 October 2025

Keywords:
Cobalt oxide
Malachite Green dye
Nanocomposite
Nickel oxide
Photocatalytic degradation

ABSTRACT

The current study involves synthesis of nickel oxide and cobalt oxide (NiO/CoO) nanocomposites at three different ratios (1:1, 1:2, and 2:1). These materials were synthesized using a co-precipitation method. The synthesized above materials were characterized by using different analytical and spectroscopic methods such as X- rays diffraction technique (XRD), scanning electron microscopy (SEM-EDX), specific surface area (BET), and Fourier transform infrared spectroscopy (FTIR). The activity of these materials was investigated by removing of Malachite Green (MG) dye from its aqueous solution by photocatalytic removal over these materials. Different photocatalytic removal conditions and parameters were conducted such as mass dosage of the used catalyst, concentration of the used dye, acidity of the solution and effect of reaction temperature. From the obtained results, the best ratio of NiO/CoO composites was (1:2) which exhibited best removal efficiency of the used dye over this composite and it was around 97%, this was obtained over using 0.2 g. of catalyst, 25 ppm of Malachite Green dye, acidity of solution (pH=6) and reaction temperature was 25 ℃. Also, the activation energy was calculated applying Arrhenius equation for this adsorption and it was around 17 KJ/mol. The dye degradation was also studied using the recovered catalysts.

How to cite this article
Hussein A., Atiyah A. Investigation of Photocatalytic Activity of the Synthesized Nickel Oxide with Cobalt Oxide Nanocomposites via Removing of Malachite Green Dye from Aqueous Solution. J Nanostruct, 2025; 15(4):1979-1993. DOI: 10.22052/JNS.2025.04.044

INTRODUCTION

The growing water contamination is mostly due to the increased demands that have fueled industrial modernization, smart living, and agricultural evolution. Polluted effluents are routinely released by industries into water supplies. Effluents are a mixture of organic and inorganic materials, including metals like lead and mercury. Improper farming practices lead to the introduction of electronic trash into municipal landfills and the deposition of heavy metals like copper and cadmium in water supplies. Water pollution from atmospheric deposition and storm runoff also rises. this includes heavy metals, inorganic pollutants, and organic contaminants [1-3].

Treatment of wastewater containing dyes using advanced oxidation processes (AOPs) shows

* Corresponding Author Email: den155.alaa.salman@uobabylon.edu.iq

This work is licensed under the Creative Commons Attribution 4.0 International License.
To view a copy of this license, visit http://creativecommons.org/licenses/by/4.0/.

greater promise. To effectively treat wastewater, AOPs must produce large amounts of oxidizing extremely reactive free radicals. One of the AOPs now under investigation for the elimination of hazardous organic pollutants from industrial effluents is heterogeneous photocatalysis. With the use of photocatalysis, organic pollutants may be completely mineralized to carbon dioxide (CO_2), water (H_2O), and mineral acids [4-6]. Under the right conditions, the reaction on the semiconductor surface in the heterogeneous photocatalytic oxidation process produces electron/hole pairs (e/h+). The water absorbed on the semiconductor surface reacts with a hole in the valence band to make hydroxyl radicals, while electrons in the conduction band reduce oxygen atoms to form peroxide radical anions, which then combine with hydrogen peroxide to form hydroxyl radicals [7]. In order to improve the photodegradation performance, several elements are doped into the photocatalyst as co-catalysts. These include noble metals, transition metals, non-metals, and metalloids (such as graphene, carbon nanotubes, and carbon quantum dots) [8].

A nanocomposite is a multi-phase material with at least one phase having dimensions in the nanoscale range. Miniaturizing a material to the nanoscale yields phase interfaces, which are crucial in improving the material's characteristics [9, 10].

Due to their excellent magnetic characteristics and prospective applications in various sectors, including as catalysis, memory storage devices, and sensors, the synthesis of magnetic NPs of Fe, Co, and Ni has gained increasing attention in recent years. They have several medical applications, including magnetic resonance imaging and heat therapy for cancer cells [11-13]. NiO has a large band gap of 3.6 to 4.0 eV and a cubic lattice structure, making it a p-type semiconductor transition metal oxide. Their capacity to transmit electrons, high chemical stability, electro catalysis, and super-capacitance have drawn a lot of interest to these NPs, which has led to extensive research into them [14]. Cobalt, a d-block transition metal, is widely employed as a pigment in paints and glazes and as a catalyst in a wide variety of chemical processes, including hydroformylation, hydrogenation, and dehydrogenation. As a component of vitamin B12, cobalt promotes healthy maintenance and aids in the treatment of anemia by stimulating the production of new red blood cells. Water-soluble nickel and cobalt compounds may induce sensitization of skin and airways, and their oxides, in particular, have allergenic potential, however exposure to amounts of cobalt commonly found in the environment is not dangerous. Nano sensors, nanoelectronics devices, and catalysts are just some of the many fields that may benefit from cobalt's exceptional electrical, catalytic, magnetic, and optical properties [15-18].

Malachite Green, also known as N-methylated di amino tri phenyl methane, is an organic chemical that consists of green-colored crystals with a metallic appearance. It is often used in many sectors involved in the production of dyes. It is one of the most potent compounds globally [19]. In aquaculture, Malachite Green (MG) is used as a fungicide, bactericide, and parasiticide. It is also used as a food additive, a disinfectant in medicine, and a color for silk, leather, paper, and other materials [20].

The current study aims to synthesize of composites of NiO/CoO at three different ratios. Then the activity of these materials would be investigated by following removal of MG dye from its aqueous solution by photocatalytic removal over these materials. this also would involve screening different conditions and factors that can affect on the photocatalytic removal efficiency.

MATERIALS AND METHODS

Used chemicals and materials

Nickel (II) nitrate hexahydrate [$Ni(NO_3)_2.6H_2O$] was obtained from (CDH) with assay 99%, Cobalt (II) nitrate hexahydrate [$Co(NO_3)_2.6H_2O$] was obtained from (Oxford Lab Chem) with assay 97-101%, sodium carbonate [Na_2CO_3] was obtained from (VWR INTERNATIONAL) with purity 99.9%, hydrochloric acid [HCl] was obtained from (BDH) with 37% and Malachite Green (MG) dye [$C_{23}H_{26}N_2O$], M.W. 346.46 $mol.g^{-1}$ was obtained from (BDH) with dye content 99%.

Synthesis a composite of nickel oxide – cobalt oxide

The co-precipitation method was utilized to synthesize the composites. This process was conducted using a mixture of $Ni(NO_3)_2.6H_2O$ and $Co(NO_3)_3.6H_2O$ (in three different ratios of 1:1, 1:2 and 2:1). This mixture was dissolved in 400 ml of deionized distilled water at a constant stirring rate and under ambient atmospheric conditions. A digital pH meter was used to adjust the pH of the final combination to the specified level. The

CC BY

solution was maintained at a temperature of (70–75) ℃ while Na_2CO_3 (1.0 M) was added drop by drop as a precipitating agent. The resulting solution's acidity was controlled to be in the range of (9.0–9.1). Then the resulted mixture was kept undisturbed for 2 hours at room temperature with a constant stirring rate. A Buchner filtration flask equipped with a vacuum pump was used to remove the contaminants from the resulting combination. After that, the material was calcined at 500℃ for 4 hours at a heating rate of 100 ℃ per minute in an air environment [21]. Fig. 1 shows the steps of synthesis of nanocomposites.

Photocatalytic removal of MG dye over NiO/CoO (1:2) nanocomposite

Photocatalytic removal of MG dye investigation of the optimal conditions for the removal of MG dye from its aqueous solution by photocatalytic removal over the synthesized catalysts (composite of nickel oxide and cobalt oxide). In this part, photocatalytic removal experiments were conducted in a closed system of the glass dual wall reactor kind, with a chiller (Julabo model EH/Germany) serving as the temperature controller. A 150 Watt of UV. Lamp (LED, China) was used for irradiation. The reaction mixture was agitated using a magnetic stirrer (Heidolph MR Hei-Standard). In each run, MG dye solution (25 ppm, 100 ml) was suspended over 0.2 g. of the used catalysts. Adsorption time was 15 min. after adsorption, the irradiation time was one hour and measured absorbance every 15 min by taking 2 mL of irradiated solution and centrifugation for 15 min in centrifuge (80-1 Electric Centrifuge). Then the absorbance of the supernatant liquids was recorded at a wavelength of 617nm using a SHIMADZU spectrophotometer double beam (UVProbe). Fig. 2 shows the structure of Malachite Green dye. The efficiency of MG dye removal (R%) was calculated using the following equation:

$$\text{Removal } \% = \frac{(A_\circ - A_t)}{A_\circ} \times 100 \quad (1)$$

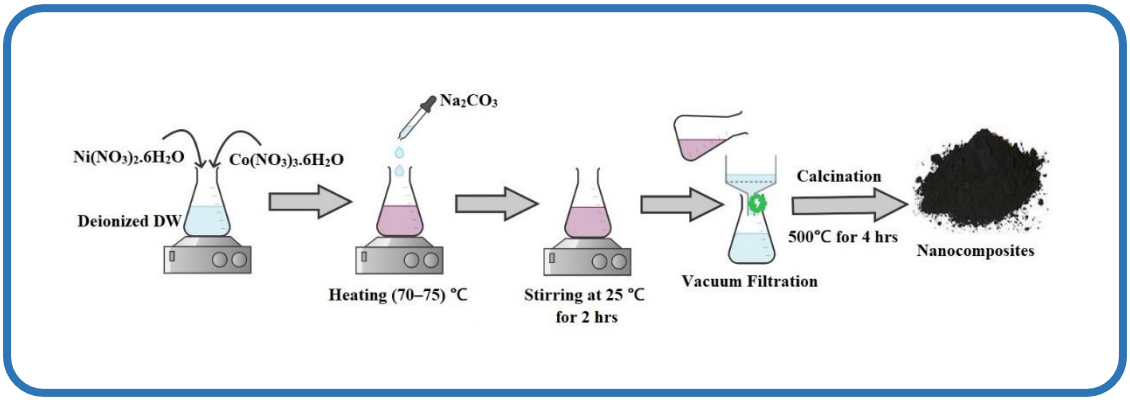

Fig. 1. The steps of synthesis of nanocomposites.

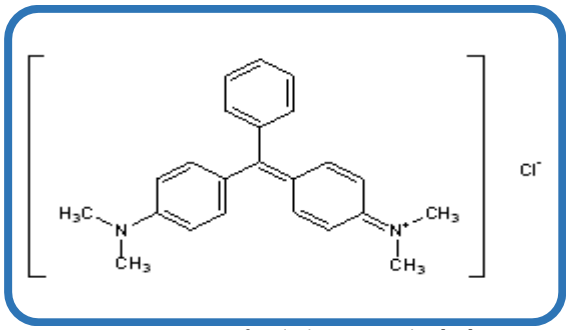

Fig. 2. Structure of Malachite Green dye [24].

CC BY

Where $A_\circ$ and A_t are the absorbance values at time zero and time t, respectively [22, 23].

UV. Vis. Spectrum of MG dye is shown in Fig. 3 to obtain λmax of dye (617 nm). Fig. 4 shows a calibration curve of MG dye in the range of concentrations from 1 to 30 ppm.

RESULTS AND DISCUSSION

Characterization of the prepared materials

X – rays Diffraction (XRD) of the synthesized materials

Crystal morphology of the synthesized materials was investigated using XRD technique. XRD patterns were conducted using PANlytical X- -rays diffraction with CuK radiation (1.542 A, 40 KV, 30 MA), in the range of 2Θ = 10-80º using a Shimadzu XRD6000 - Japan. Fig. 5 illustrates XRD patterns of composites for NiO/CoO in three different ratios, 1:1, 1:2 and 2:1. In the XRD of nano- composite film, peaks observed at 2θ = 36.43°, 44.51° and 64.84° can be assigned to (311), (400), and (440) planes of $NiCo_2O_4$ in the composite (JCPDS card no. 20-0781) [25, 26] In order to determine the particle size, the Scherrer formula was used. The formula $D = k \lambda / \beta \cos\theta$ takes into account the following variables: k, the size of the crystallite (in nanometers), the wavelength of the x-ray radiation (Cu-Kα = 0.1541 nm), β, the full width at half maximum (FWHM) of the intense and wide peaks, and θ, the Bragg's or diffraction angle [27]. From the obtained results, the crystallite sizes were around 15 nm for NiO/CoO (1:1), 17 nm for NiO/CoO (2:1) and 13 nm for NiO/CoO (1:2). So that, all the synthesized materials in the present study are full in nanometer scale.

Fourier Transform Infrared Spectroscopy (FTIR) for the synthesized materials

FTIR spectra for the synthesized three samples of composites of NiO/CoO are shown in Fig. 6. The nanocomposite's FTIR spectra revealed that the precursor exhibited the fundamental absorption frequency bands between 4000 and 400 cm-1. Hydrogen-bonded hydroxyl groups at 3418 cm^{-1} and the bending vibration of water molecules at 1618 cm-1 are two of the most prominent bands in the spectrum. Metal oxide vibrations were thought to be responsible for the weak bands seen at 538cm^{-1} and 429 cm^{-1} [28-30].

Scanning Electron Microscopy (SEM) and Energy Dispersive X-rays (EDX) for the synthesized materials

Surface morphology of the synthesized materials was investigated using SEM technique and the obtained images are shown in Fig. 7. From these images it can be seen that, in all samples a spherical shape for the three samples with relative aggregation for these particles was seen. Besides that, all samples have an average particle size to in the range from 21 nm to 34 nm.

Fig. 8A, B and C shows EDX results for the synthesized composites, NiO/CoO (1:1) (A), (2:1)

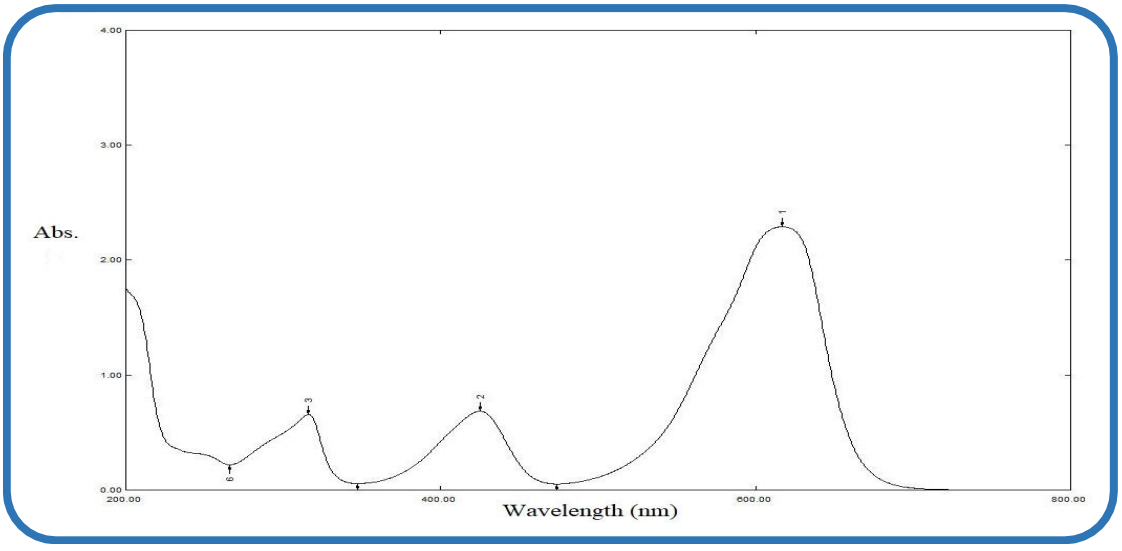

Fig. 3. UV. Vis. Spectrum of (20 ppm) MG dye, λmax 617 nm.

CC BY

(B) and (1:2) (C). These spectra show elemental composition with weight percent of these materials. Fig. 8A, shows elemental composition of composites of nickel oxide and cobalt oxide, NiO/CoO (1:1), it shows a percent of 33.4 wt% of nickel, 23.9 wt% of cobalt and 26.2 wt% of oxygen. Fig. 8B, shows elemental composition of composites of nickel oxide and cobalt oxide, NiO/CoO (2:1), it consists of 12.2 wt% of nickel, 12.3wt% of cobalt and 41.8 wt% of oxygen. Fig. 8C, shows elemental composition of a composite of nickel oxide and cobalt oxide, NiO/CoO (1:2), it consists of 22.9 wt% of nickel, 41.3 wt% of cobalt and 25.5 wt% of oxygen. In general, these results confirm presence of the proposed element in each sample.

Specific surface areas (BET) for the prepared

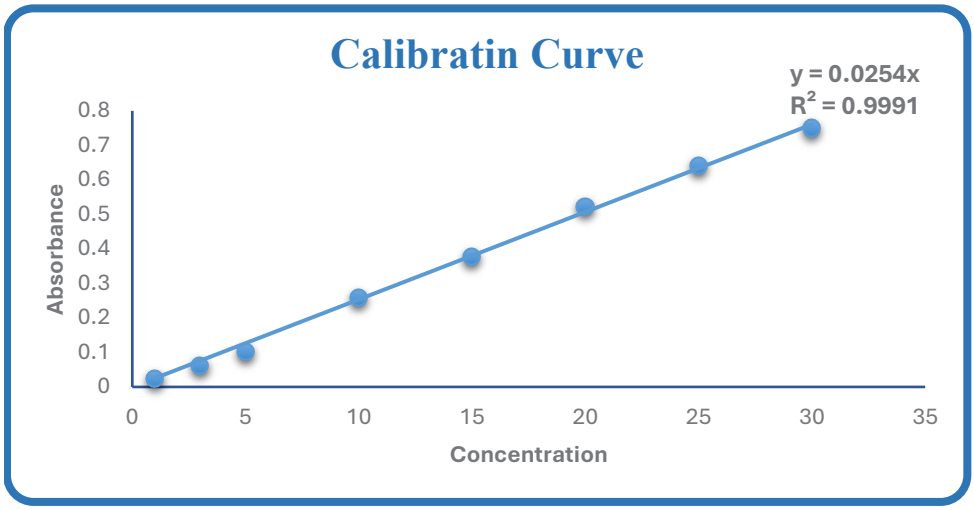

Fig. 4. Calibration curve of MG dye (1 – 30) ppm.

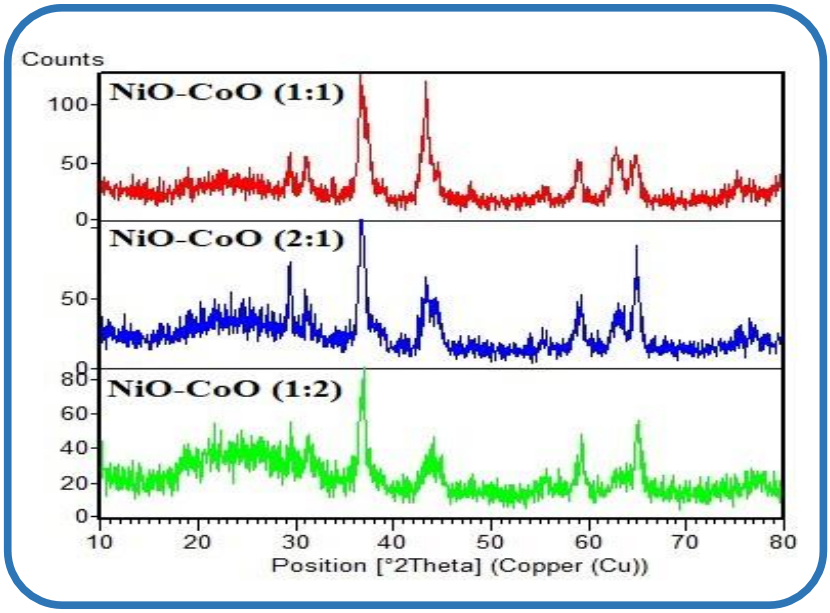

Fig. 5. XRD patterns for composites NiO/CoO.

CC BY

materials are shown in Table 1. From these results, it can be seen that, there was a reduction in the specific surface area for synthesized composites of nickel oxide and cobalt oxide in the three ratios (1:1, 2:1 and 1:2).

The BET specific surface area for the composite NiO/CoO in a ratio of (1:2), there was an increase in surface area for this composite in comparison with other composites in other ratios. This can be attributed to the role of high ratio of cobalt oxide in this composite to increase porosity of the resulted material which lead to relative increase its specific surface area for this composite [31].

Photocatalytic removal of MG dye over NiO/CoO composites

To investigate photocatalytic activity of the three different ratios of the synthesized

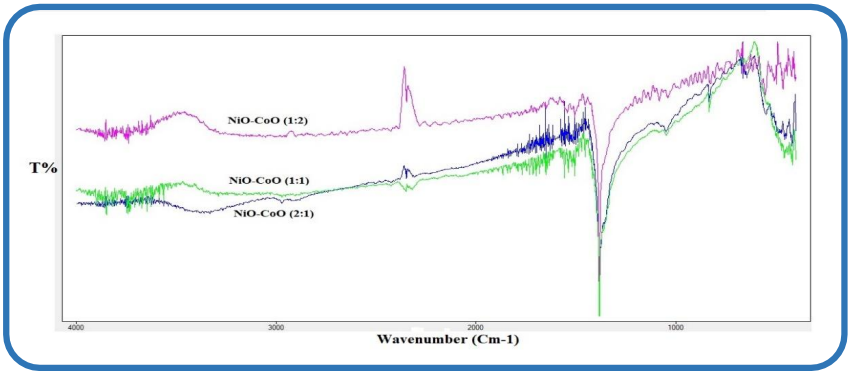

Fig. 6. FTIR spectra for composites of NiO/CoO.

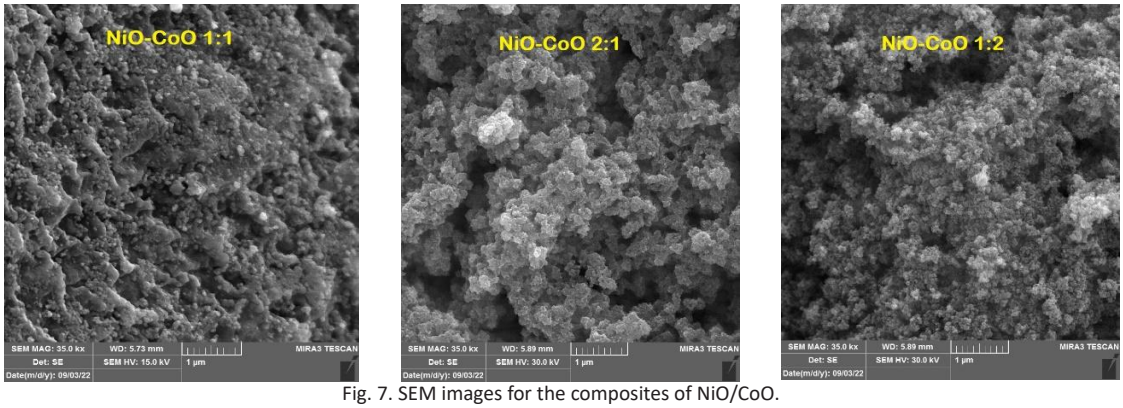

Fig. 7. SEM images for the composites of NiO/CoO.

Table 1. BET surface area of synthesized composites of nickel oxide and cobalt oxide.

Catalysts	BET (m^2 / g)
NiO/CoO (1:1)	8.5103
NiO/CoO (2:1)	8.4250
NiO/CoO (1:2)	14.0445

CC BY

nanomaterials, a series of experiments were conducted using same amount of each one, and some other photocatalytic conditions including dye concentration, temperature of solution, pH of solution, and dosage of the used catalyst, which was one hour of photoreaction for each run. The obtained results are presented in Fig. 9. From the obtained results, it can be seen that, the optimum removal efficiency was achieved over NiO/CoO composites (1:2) ratio. This is most likely due to its large specific surface area and outstanding surface characteristics when compared to other synthesized nanomaterials. This means that, NiO/CoO ratio (1:2) would be expected to be a best photocatalyst among the other synthesized nanomaterials that were synthesized in this study.

Effect dosage of the used photocatalyst on the efficiency of MG dye removal

To investigate effect of the used masses of the catalyst on the efficiency of MG dye removal over the best used catalyst which was NiO/CoO ratio (1:2). A series of dosages of NiO/CoO ratio (1:2) in the range of 0.05 to 0.3 g. were conducted under a fixed other reaction parameter. The obtained results are presented in Fig. 10. From the obtained results, it was found that, the best removal efficiency was attained with 0.2 g. of the used catalyst, and the removal efficiency was

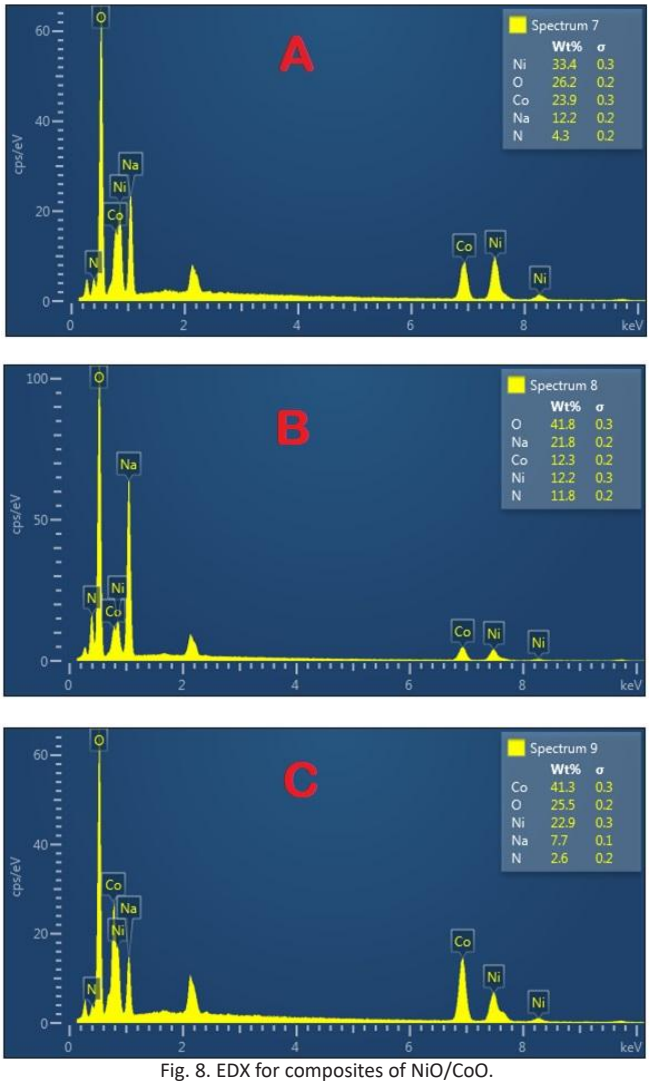

Fig. 8. EDX for composites of NiO/CoO.

CC BY

increased as the amount of catalyst was increased. According to the results, the efficiency of dye removal improved with increasing catalyst dosage. Dye removal efficiency drops down significantly beyond a threshold value of the catalyst dosage (0.2 g). Since there were originally few catalyst particles available to absorb light photons at low concentrations, the ratio of incoming photons to catalyst particles will be directly proportional. The principles of photochemistry, which account for these findings, are compatible with this. The catalyst particles will form an inner filter that prevents light from reaching the other side of the reaction mixture when the concentration of catalyst is high and the intensity of the light is constant [32]. So that, from the obtained results in this study it was found that, 0.2 g was the optimal dose for in this study which gives a maximum

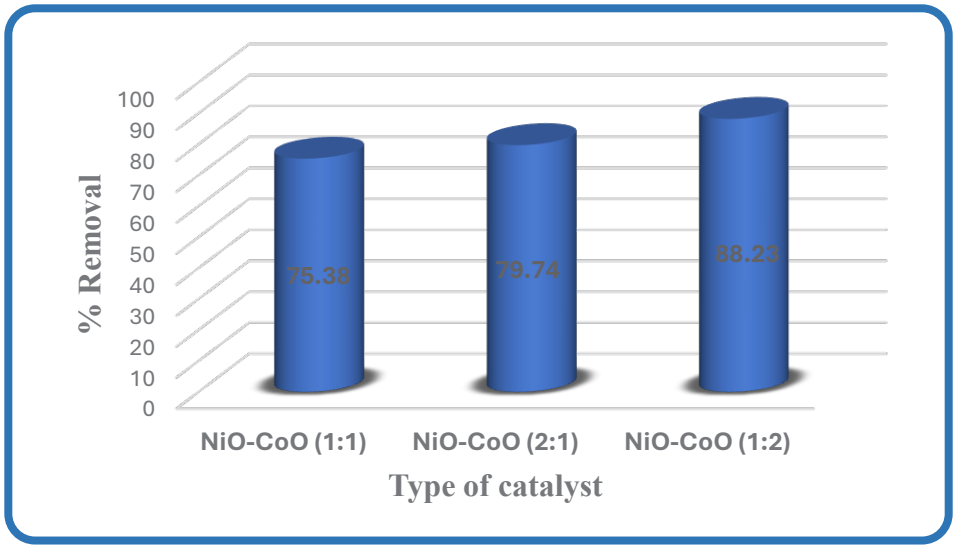

Fig. 9. Removal efficiency of MG dye over the three synthesized nanocomposites.

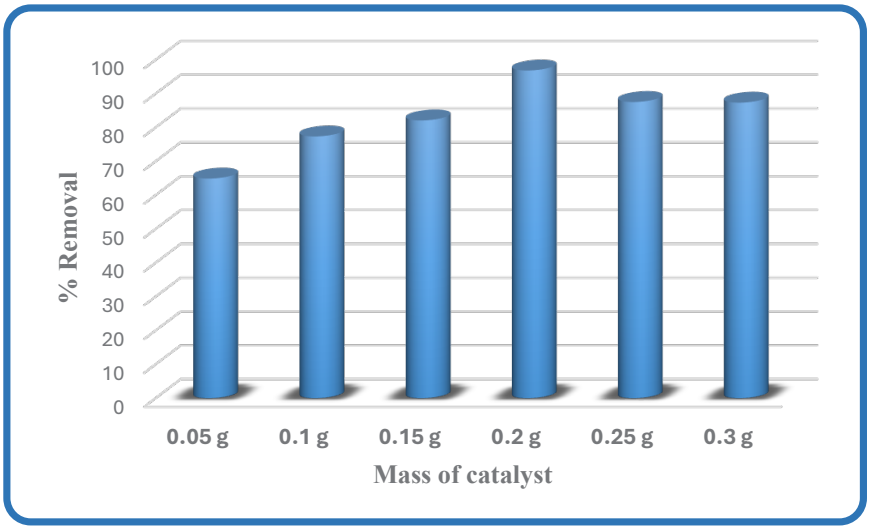

Fig. 10. Effect of using different dosages of NiO/CoO (1:2) on the efficiency of MG removal by photocatalytic process.

CC BY

removal efficiency for the used which was around 97%.

Effect of MG dye concentration on the efficiency of its photocatalytic removal over NiO/CoO (1:2) nanocomposite

The effect of dye concentration on the efficiency of its photocatalytic removal over NiO/CoO (1:2) was investigated over 0.2 g. of this composite with fixation of all other reaction conditions with variation MG dye concentration only. To conduct this factor, a series of dye concentrations were investigated from (5 to 30) ppm, over a fixed amount (0.2) g. of the used catalyst. The remaining concentration of dye after photocatalytic removal was recorded according to the previously established calibration curve for the dye. The obtained results are presented in Fig. 11. From these results, it can be seen that, from 5 ppm up to 25 ppm, the rate of MG dye removal was increased as dye concentration increased. This observation is probably due to occupation of active sites at the surface of the used catalyst partially or completely covered by dye molecules. [33]. After this point, dye concentrations more than (25 ppm), dye removal efficiency was reduced linearly with increasing of dye concentrations above this value. One possible explanation for this phenomenon is that there are more dye molecules available for excitation and energy transfer when the initial dye concentrations are increased. In addition, the rate of molecular diffusion might be adversely affected by an increase in concertation since it can cause the solution's viscosity to rise [34]. According to the observations, 25 ppm was chosen to be as an optimum dye concentration under these circumstances.

Effect of pH of MG dye solution on the efficiency of its removal

In order to investigate the effect of pH of dye solution on the efficiency of photocatalytic removal over NiO/CoO (1:2). A series of experiments were performed with keeping all other photocatalytic conditions constant with variation only pH of dye solution. The effect of pH was screened in the range of (pH=2 – 12). Adjusting of pH of solution was conducted by using hydrochloric acid and sodium hydroxide to adjust pH of dye solution at a desired value. The obtained results are presented in Fig. 12. From the obtained results, it is clear that, MG dye removal efficiency was increased with increase acidity from pH = 2 to pH = 6 to reach maximum removal efficiency. After this point, dye removal efficiency was reduced steadily from a neutral (7) to a high basic medium (pH=12). These observations can be related to the effect of pH of solution on the net charge of the

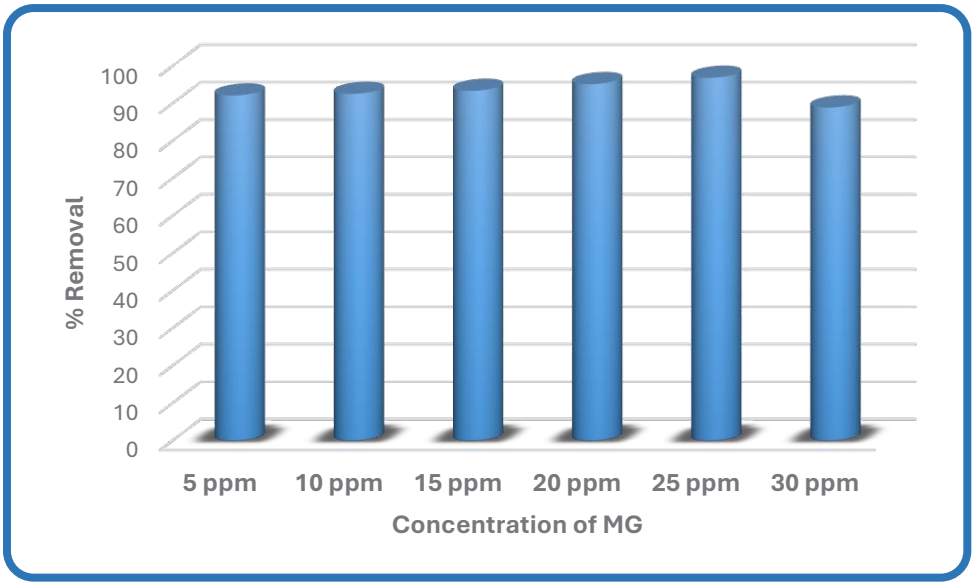

Fig. 11. Effect of MG dye concentration on the efficiency of its removal over NiO/CoO (1:2).

CC BY

surface of the used catalyst. In this context, the acidity or the basicity of the dye solution would effect on the catalyst's net charge [35]. In general, the nanocomposite's negative surface at high pH encourages the adsorption of cations, leading to electrostatic attraction. However, at acidic pH, the nanocomposite's surface becomes positively charged as a result of protonation, encouraging the adsorption of anions. Additionally, hydroxyl radical generation is highest in the alkaline pH range. Peroxide radicals are created when electrons oxidize oxygen molecules. Hydroxyl radicals, formed when this radical combines with atmospheric hydrogen, are important for

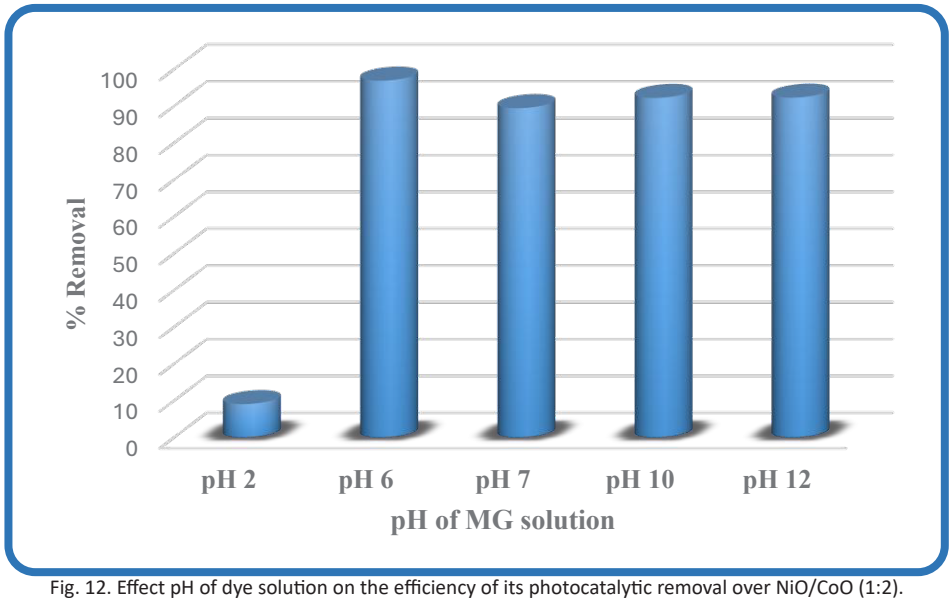

Fig. 12. Effect pH of dye solution on the efficiency of its photocatalytic removal over NiO/CoO (1:2).

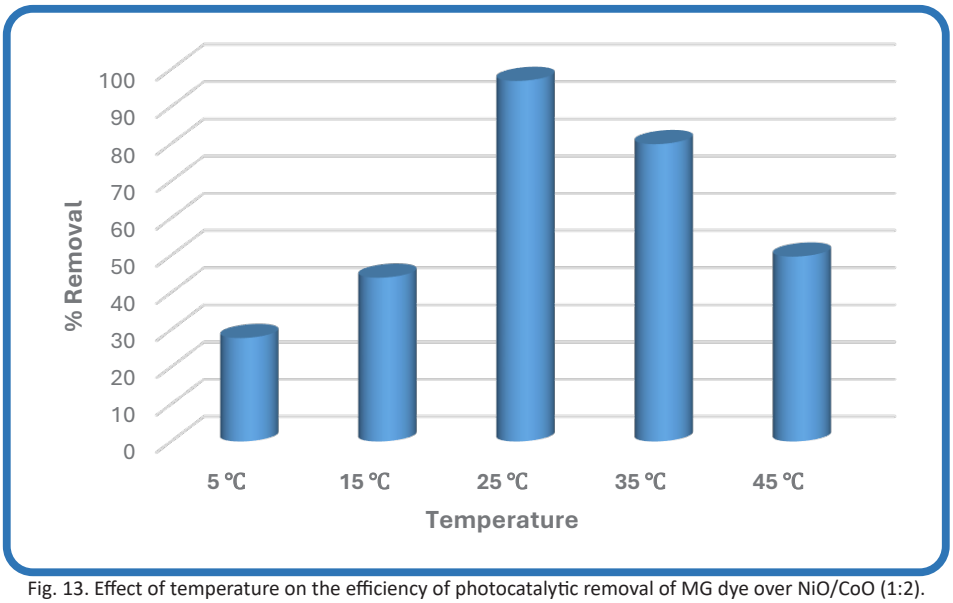

Fig. 13. Effect of temperature on the efficiency of photocatalytic removal of MG dye over NiO/CoO (1:2).

photocatalytic activity [36].

Effect of temperature on the efficiency of MG dye removal over NiO/CoO (1:2)

To investigate effect of temperature on the efficiency of MG dye removal over the used NiO/CoO (1:2) catalyst, a series of experiments were conducted in the range of temperature from 5 ℃ to 45℃. All other photocatalytic conditions were kept constant for each case including using 0.2 g. mass of catalyst, same dye concentration (25) ppm, and using same photoreaction period of one hour for each case. The obtained results are presented in Fig. 13. From the obtained results, it was found that, when the temperature was raised from 5 to 25 ℃, the dye was removed more effectively. Dye removal effectiveness then decreased with further increases in reaction temperature (over 25 ℃). Surface degradation and reactant adsorption are more rapid at low temperatures; hence product desorption restricts the reaction. However, as the temperature is increased, the deciding step shifts to the adsorption of the dye onto the surface of NiO/CoO (1:2). Increased dissolved oxygen at higher temperatures likely contributes to a lower rate constant, which in turn reduces the adsorptive capacity. Therefore, the ideal reaction temperature in this investigation was around 25 ℃ under these conditions [37-39].

Rate constant for photocatalytic removal of MG dye over NiO/CoO (1:2) was estimated by plotting $\ln A_o/At$ as a function of time assuming pseudo first order kinetics, and the obtained results are presented in Fig. 14 and the obtained values of rate constants are presented in Table 2. Calculation of reaction rate constant ($Kmin^{-1}$) pseudo first order)

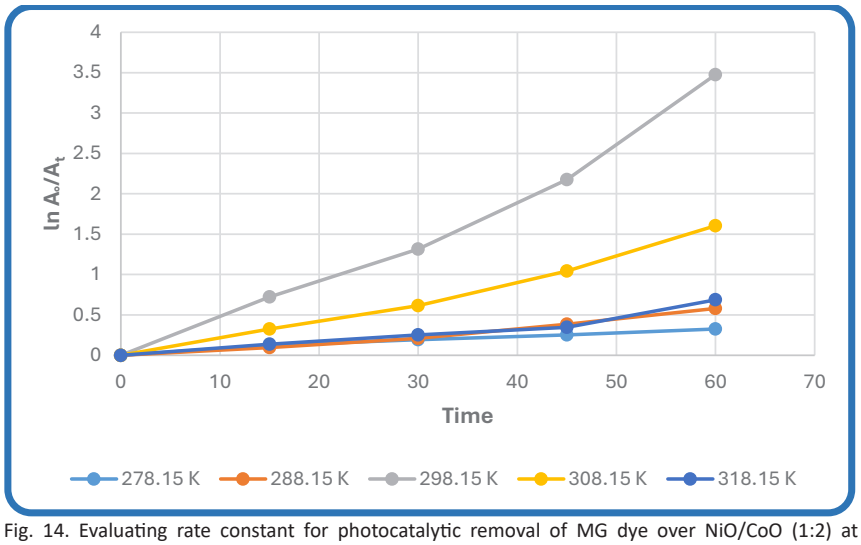

Fig. 14. Evaluating rate constant for photocatalytic removal of MG dye over NiO/CoO (1:2) at different temperatures.

Table 2. rate constant values for photocatalytic removal of MG dye over NiO/CoO (1:2) at different temperatures.

Temperature (K)	Reaction rate constant K (min^{-1})
278.15	0.0057
288.15	0.0089
298.15	0.0529
308.15	0.0247
318.15	0.0098

CC BY

of photocatalytic removal of MG dye over NiO/CoO (1:2) catalyst are presented in Table 2.

Calculation of activation energy for photocatalytic removal of MG dye over NiO/CoO (1:2)

Activation energy (Ea) for photocatalytic removal of MG dye over NiO/CoO (1:2) was calculated by applying Arrhenius Eq. 2. The obtained results are summarized in Table 3 and are plotted in Fig. 15.

$$\ln K = \ln A - \frac{Ea}{RT} \quad (2)$$

Where K reaction rate constant (min^{-1}), A is Arrhenius factor, Ea is activation energy (kJ/mol), R is a universal gas constant = 8.314 (J/mol.K) and T is temperature (K) [40].

From the obtained results, the activation energy that was estimated by applying Arrhenius equation was around 16.7585 KJ/mol. Generally, the obtained result in our current study is in a good agreement with the previous works regarding to this issue. This value of activation energy is considered to be associated with electron transfer from valence band to the conduction band of the used photocatalyst [41].

Possible degradation pathway of malachite green

The proposed pathways for the photocatalytic degradation of MG dye over the used materials are presented in Fig. 16. In this context, MG dye can be oxidized by hydroxyl radical to produce 4-(dimethyla- mino) cyclohexa-2,5-dien-1-yl)-4-

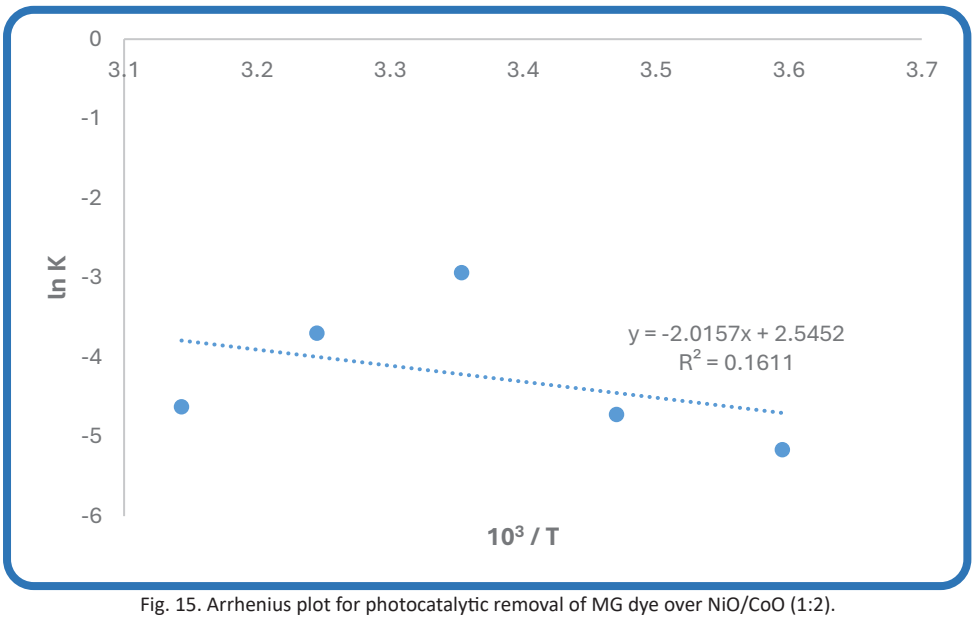

Fig. 15. Arrhenius plot for photocatalytic removal of MG dye over NiO/CoO (1:2).

Table 3. Photocatalytic removal's temperatures and rate constants for photocatalytic removal of MG dye over NiO/CoO (1:2).

Temperature (K)	Reaction rate constant K (min^{-1})	1000/T	Ln K
278.15	0.0057	3.595182456	-5.16729
288.15	0.0089	3.470414715	-4.7217
298.15	0.0529	3.354016435	-2.93935
308.15	0.0247	3.245172805	-3.70095
318.15	0.0098	3.14317146	-4.62537

CC BY

(dimethylamino)phenyl)-methanol. Both routes (a) and (b) were then used to break down this molecule. Both directions of breakdown of the big molecules resulted in the production of organic acids like maleic acid, which oxidized to oxalic acid. Finally, the tiny organic acids were mineralized to carbon dioxide and H_2O products [42].

Recyclability of catalyst

Racialization of the used photocatalyst was performed via separation of the used materials by centrifugation, then it was washed with de-ionized distilled water for several times with carefully drying. Then the recycled materials were applied under the same conditions of experimentation, the MG dye was degraded utilizing the recovered photocatalyst. For a period of one hour of irradiation, removal efficiency of dye over the original NiO/CoO (1:2) was around 97%. On the other hand, removal efficiency for

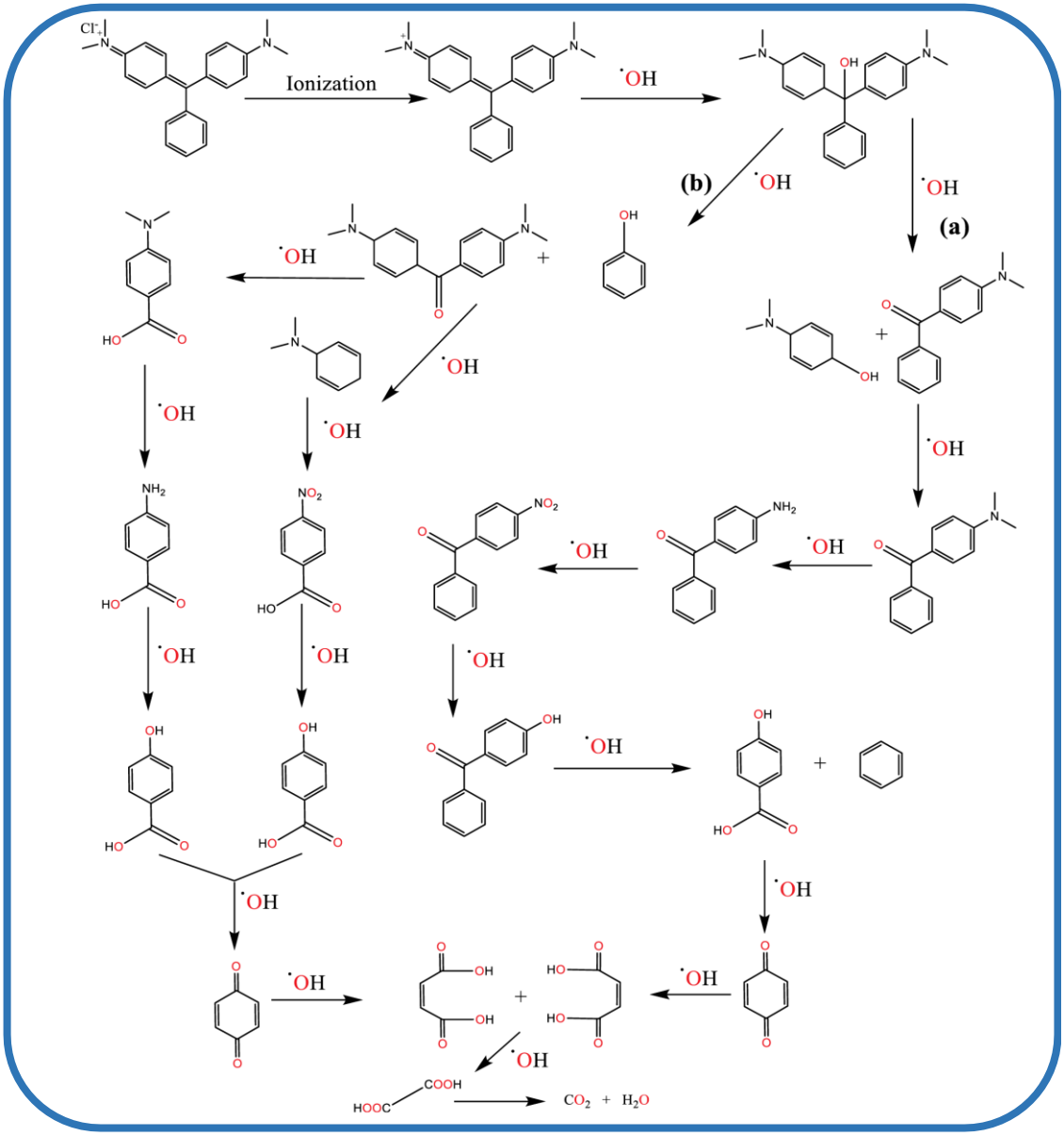

Fig. 16. Schematic diagram for the pathway of photocatalytic degradation of MG [42].

CC BY

the used dye over the same recycled photocatalyst was around 65%. This drop in the activity of the used photocatalyst is probably associated with the still occupation of active sites of the catalyst with strongly adsorbed of reacting species or probably with some of produced species even when it was activated by washing with deionized distilled water. So that, active sites of the surface were partially or completely blocked with these species. This may lead to reduce photocatalytic activity for the recovered photocatalyst in comparison with the original/fresh photocatalyst under the same reaction conditions [43-45].

CONCLUSION

In this study, three composites of nickel oxide and cobalt oxide were synthesized in three different ratios. Then the activity of these materials was investigated by following removal of MG dye from its aqueous solution by photocatalytic removal over these materials. The obtained results showed that, the best removal efficiency was achieved over NiO/CoO (1:2) ratio under using 0.2 g. of the catalyst, 25 ppm of MG dye, acidity of solution (pH=6) and temperature solution equal to 25℃. The optimum removal efficiency was achieved under these conditions was around 97% by photocatalytic removal of MG dye over NiO/CoO (1:2) ratio. Also, the activation energy for photocatalytic removal of MG dye over this catalyst was conducted and it was around 17 kJ/mol. The dye degradation was also studied using the same recovered catalyst using simple activation approach and the removal efficiency was around 65%.

ACKNOWLEDGEMENTS

The authors would like thank University of Babylon, College of Science for their fund and support for this work.

CONFLICT OF INTEREST

The authors declare that there is no conflict of interests regarding the publication of this manuscript.

REFERENCES

1. Babu Ponnusami A, Sinha S, Ashokan H, V Paul M, Hariharan SP, Arun J, et al. Advanced oxidation process (AOP) combined biological process for wastewater treatment: A review on advancements, feasibility and practicability of combined techniques. Environ Res. 2023;237:116944.
2. Bracamontes-Ruelas AR, Reyes-Vidal Y, Irigoyen-Campuzano JR, Reynoso-Cuevas L. Simultaneous Oxidation of Emerging Pollutants in Real Wastewater by the Advanced Fenton Oxidation Process. Catalysts. 2023;13(4):748.
3. Vasilachi I, Asiminicesei D, Fertu D, Gavrilescu M. Occurrence and Fate of Emerging Pollutants in Water Environment and Options for Their Removal. Water. 2021;13(2):181.
4. Priyanka, Srivastava VC. Photocatalytic Oxidation of Dye Bearing Wastewater by Iron Doped Zinc Oxide. Industrial and Engineering Chemistry Research. 2013;52(50):17790-17799.
5. Zangeneh H, Zinatizadeh AAL, Habibi M, Akia M, Hasnain Isa M. Photocatalytic oxidation of organic dyes and pollutants in wastewater using different modified titanium dioxides: A comparative review. Journal of Industrial and Engineering Chemistry. 2015;26:1-36.
6. Dhatshanamurthi P, Shanthi M. Enhanced photocatalytic degradation of azo dye in aqueous solutions using Ba@Ag@ZnO nanocomposite for self-sensitized under sunshine irradiation. Int J Hydrogen Energy. 2017;42(8):5523-5536.
7. Shinde SS, Bhosale CH, Rajpure KY. Photocatalytic degradation of toluene using sprayed N-doped ZnO thin films in aqueous suspension. J Photochem Photobiol B: Biol. 2012;113:70-77.
8. Koe WS, Lee JW, Chong WC, Pang YL, Sim LC. An overview of photocatalytic degradation: photocatalysts, mechanisms, and development of photocatalytic membrane. Environmental Science and Pollution Research. 2019;27(3):2522-2565.
9. Omanović-Mikličanin E, Badnjević A, Kazlagić A, Hajlovac M. Nanocomposites: a brief review. Health and Technology. 2019;10(1):51-59.
10. Khalifeh S. Introduction to Polymers for Electronic Engineers. Polymers in Organic Electronics: Elsevier; 2020. p. 1-31.
11. Imran Din M, Rani A. Recent Advances in the Synthesis and Stabilization of Nickel and Nickel Oxide Nanoparticles: A Green Adeptness. Int J Anal Chem. 2016;2016:1-14.
12. Hao R, Xing R, Xu Z, Hou Y, Gao S, Sun S. Synthesis, Functionalization, and Biomedical Applications of Multifunctional Magnetic Nanoparticles. Adv Mater. 2010;22(25):2729-2742.
13. Narender SS, Varma VVS, Srikar CS, Ruchitha J, Varma PA, Praveen BVS. Nickel Oxide Nanoparticles: A Brief Review of Their Synthesis, Characterization, and Applications. Chemical Engineering and Technology. 2022;45(3):397-409.
14. Din MI, Nabi AG, Rani A, Aihetasham A, Mukhtar M. Single step green synthesis of stable nickel and nickel oxide nanoparticles from Calotropis gigantea : Catalytic and antimicrobial potentials. Environmental Nanotechnology, Monitoring and Management. 2018;9:29-36.
15. Iravani S, Varma RS. Sustainable synthesis of cobalt and cobalt oxide nanoparticles and their catalytic and biomedical applications. Green Chem. 2020;22(9):2643-2661.
16. Faucon M-P, Pourret O, Lange B. Element Case Studies: Cobalt. Mineral Resource Reviews: Springer International Publishing; 2020. p. 385-391.
17. Egorova KS, Ananikov VP. Toxicity of Metal Compounds: Knowledge and Myths. Organometallics. 2017;36(21):4071-4090.
18. Yu Y, Mendoza-Garcia A, Ning B, Sun S. Cobalt-Substituted Magnetite Nanoparticles and Their Assembly into Ferrimagnetic Nanoparticle Arrays. Adv Mater. 2013;25(22):3090-3094.

CC BY

19. Jabeen S, Ganie AS, Bala S, Khan T. Photocatalytic Degradation of Malachite Green Dye via An Inner Transition Metal Oxide-Based Nanostructure Fabricated through a Hydrothermal Route. IOCN 2023; 2023/05/05: MDPI; 2023. p. 5.
20. Amiri-Hosseini S, Hashempour Y. Photocatalytic removal of Malachite green dye from aqueous solutions by nano-composites containing titanium dioxide: A systematic review. Environmental Health Engineering and Management. 2021;8(4):295-302.
21. Mohammad EJ, Lafta AJ, Kahdim SH. Photocatalytic removal of reactive yellow 145 dye from simulated textile wastewaters over supported (Co, $Ni)_3O_4/Al_2O_3$ co-catalyst. Polish Journal of Chemical Technology. 2016;18(3):1-9.
22. Jasrotia R, Suman, Verma A, Verma R, Godara SK, Ahmed J, et al. Photocatalytic degradation of malachite green pollutant using novel dysprosium modified Zn–Mg photocatalysts for wastewater remediation. Ceram Int. 2022;48(19):29111-29120.
23. Verma M, Mitan M, Kim H, Vaya D. Efficient photocatalytic degradation of Malachite green dye using facilely synthesized cobalt oxide nanomaterials using citric acid and oleic acid. Journal of Physics and Chemistry of Solids. 2021;155:110125.
24. Swan NB, Zaini MAA. Adsorption of Malachite Green and Congo Red Dyes from Water: Recent Progress and Future Outlook. Ecological Chemistry and Engineering S. 2019;26(1):119-132.
25. Siwatch P, Sharma K, Manyani N, Kang J, Tripathi SK. Characterization of nanostructured nickel cobalt oxide-polyvinyl alcohol composite films for supercapacitor application. J Alloys Compd. 2021;872:159409.
26. Siwatch P, Sharma K, Tripathi SK. Facile synthesis of $NiCo_2O_4$ quantum dots for asymmetric supercapacitor. Electrochimica Acta. 2020;329:135084.
27. Mustapha S, Ndamitso MM, Abdulkareem AS, Tijani JO, Shuaib DT, Mohammed AK, et al. Comparative study of crystallite size using Williamson-Hall and Debye-Scherrer plots for ZnO nanoparticles. Advances in Natural Sciences: Nanoscience and Nanotechnology. 2019;10(4):045013.
28. Etape EP, Agbor OE, Namondo BV, Etape RT-D, Enongene EE, Kahbit BE. Green Synthesis, Morphological and Magnetic Studies of Pure Nickel and Cobalt-doped Nickel Oxide/Nickel Hydroxide ($Co_xNi_{1-x}O/Ni(OH)_2$) Nano Composites. Chemical and Materials Sciences: Research Findings Vol. 4: BP International; 2025. p. 87-107.
29. Khalaj M, Golkhatmi SZ, Sedghi A. High-performance supercapacitor electrode materials based on chemical co-precipitation synthesis of nickel oxide (NiO)/cobalt oxide (Co_3O_4)-intercalated graphene nanosheets binary nanocomposites. Diamond Relat Mater. 2021;114:108313.
30. Harilal M, Krishnan SG, Vijayan BL, Venkatashamy Reddy M, Adams S, Barron AR, et al. Continuous nanobelts of nickel oxide–cobalt oxide hybrid with improved capacitive charge storage properties. Materials and Design. 2017;122:376-384.
31. Abdolahi B, Gholivand MB, Shamsipur M, Amiri M. Engineering of nickel-cobalt oxide nanostructures based on biomass material for high performance supercapacitor and catalytic water splitting. International Journal of Energy Research. 2021;45(9):12879-12897.
32. Mohammad EJ, Kareem MM, Atiyah AJ. Photocatalytic oxidation of butan-2-ol over multi walled carbon nanotubes/cobalt phthalocynanine composites. Bull Chem Soc Ethiop. 2022;36(1):197-207.
33. Yadav R, Chundawat TS, Rawat P, Rao GK, Vaya D. Photocatalytic degradation of malachite green dye by ZnO and ZnO–β-cyclodextrin nanocomposite. Bull Mater Sci. 2021;44(4).
34. Elkady MF, Hassan HS. Photocatalytic Degradation of Malachite Green Dye from Aqueous Solution Using Environmentally Compatible Ag/ZnO Polymeric Nanofibers. Polymers. 2021;13(13):2033.
35. Mostafa EM, Amdeha E. Enhanced photocatalytic degradation of malachite green dye by highly stable visible-light-responsive Fe-based tri-composite photocatalysts. Environmental Science and Pollution Research. 2022;29(46):69861-69874.
36. Rangkooy HA, Jahani F, Siahi Ahangar A. Photocatalytic removal of xylene as a pollutant in the air using ZnO-activated carbon, TiO_2-activated carbon, and TiO_2/ZnOactivated carbon nanocomposites. Environmental Health Engineering and Management. 2020;7(1):41-47.
37. Soares ET, Lansarin MA, Moro CC. A study of process variables for the photocatalytic degradation of rhodamine B. Brazilian Journal of Chemical Engineering. 2007;24(1):29-36.
38. Reza KM, Kurny ASW, Gulshan F. Parameters affecting the photocatalytic degradation of dyes using TiO2: a review. Applied Water Science. 2015;7(4):1569-1578.
39. Mehrotra K, Yablonsky GS, Ray AK. Macro kinetic studies for photocatalytic degradation of benzoic acid in immobilized systems. Chemosphere. 2005;60(10):1427-1436.
40. Tekin D, Kiziltas H, Ungan H. Kinetic evaluation of ZnO/TiO_2 thin film photocatalyst in photocatalytic degradation of Orange G. J Mol Liq. 2020;306:112905.
41. Cs3Bi2Br9 Nanodots Stabilized on Defective BiOBr Nanosheets by Interfacial Chemical Bonding: Modulated Charge Transfer for Photocatalytic C(sp3)H Bond Activation. American Chemical Society (ACS).
42. Saad AM, Abukhadra MR, Abdel-Kader Ahmed S, Elzanaty AM, Mady AH, Betiha MA, et al. Photocatalytic degradation of malachite green dye using chitosan supported ZnO and Ce–ZnO nano-flowers under visible light. J Environ Manage. 2020;258:110043.
43. Naz F, Saeed K. Synthesis of barium oxide nanoparticles and its novel application as a catalyst for the photodegradation of malachite green dye. Applied Water Science. 2022;12(6).
44. Saeed K, Khan I, Sadiq M. Synthesis of graphene-supported bimetallic nanoparticles for the sunlight photodegradation of Basic Green 5 dye in aqueous medium. Sep Sci Technol. 2016;51(8):1421-1426.
45. Rehman WU, Khattak MTN, Saeed A, Shaheen K, Shah Z, Hussain S, et al. Co_3O_4/NiO nanocomposite as a thermocatalytic and photocatalytic material for the degradation of malachite green dye. Journal of Materials Science: Materials in Electronics. 2023;34(1).

CC BY